Three-dimensional nanostructuring in YIG ferrite with femtosecond laser

Tomohiro Amemiya,[1,*] Atsushi Ishikawa,[2] Yuya Shoji,[3] Pham Nam Hai,[4] Masaaki Tanaka,[4] Tetsuya Mizumoto,[3] Takuo Tanaka,[2] and Shigehisa Arai[1,3]

[1]*Quantum Nanoelectronics Research Center, Tokyo Institute of Technology, Tokyo 152-8552, Japan*

[2]*Metamaterials Laboratory, RIKEN, Wako, Saitama 351-0198, Japan*

[3]*Department of Electrical and Electronic Engineering, Tokyo Institute of Technology, Tokyo 152-8552, Japan*

[4]*Department of Electrical Engineering and Information Systems, The University of Tokyo, Tokyo 113-8656, Japan*

**Corresponding author: amemiya.t.ab@m.titech.ac.jp*

Received October 18, 2013; revised December 1, 2013; accepted December 2, 2013; posted December 4, 2013 (Doc. ID 199770); published January 3, 2014

With the goal of creating magneto-optical devices, we demonstrated forming nanostructures inside a substrate of cerium-substituted yttrium iron garnet (Ce:YIG) by means of direct laser writing. Laser irradiation changed both the optical and magnetic properties of Ce:YIG. The measurements showed that the refractive index was increased by 0.015 (about 0.7% change) and the magnetization property was changed from hard to soft to decrease the coercivity. This technology enables the formation of 3-dimensional optical and magnetic nanostructures in YIG and will contribute to the development of novel devices for optical communication and photonic integration. © 2014 Optical Society of America

OCIS codes: (320.2250) Femtosecond phenomena; (160.3820) Magneto-optical materials; (130.3130) Integrated optics materials; (230.3240) Isolators.

http://dx.doi.org/10.1364/OL.39.000212

Cerium-substituted yttrium iron garnet ($Ce_xY_{3-x}Fe_5O_{12}$: Ce:YIG) is a ferrimagnetic ceramic material with a large Faraday rotation and high transparency for infrared light wavelengths over 600 nm [1,2]. Because of its good figure of merit defined by $|\theta_F|T^2$ (θ_F is the Faraday rotation and T is the transmittance) [3], Ce:YIG has been widely used for Faraday rotators, microwave filters, and various nonlinear optical devices. In addition to these existing applications, Ce:YIG can be used to make nonreciprocal waveguide devices to break the time-reversal symmetry of light propagation in photonic integrated circuits (PICs) [4,5]. For example, efficient unidirectional devices for PICs, such as the modified Mach–Zehnder interferometers [6,7] and ring resonators [8,9], have been created using the nonreciprocal phase-shift effect observed in optical waveguides combined with Ce:YIG.

Although Ce:YIG has many potential applications in PICs, it is not very compatible with PICs. To make functional PICs, we had to join many Ce:YIG elements with semiconductor waveguides on PICs. However, existing YIG joining uses either an adhesive agent or plasma-assisted direct bonding [10,11], and neither of these are sufficient for mechanical, chemical, and thermal durability. To make reliable PICs, we have to decrease the number of joined parts and therefore decrease the number of YIG elements. So, let us consider incorporating two or more YIG elements together with attached optical waveguides into a piece of YIG material. For this purpose, here we first report a 3-dimensional (3D) nanostructuring of Ce:YIG with a femtosencond laser.

Direct 3D writing with intense femtosecond laser pulses has been used to form nanostructures in transparent materials such as glasses and polymers [12–16]. In this Letter, we apply this technology to ferrimagnetic ceramic materials, using Ce:YIG as an example. We show that laser irradiation of Ce:YIG modifies both the optical and magnetic properties of the irradiated areas. Because of the nonlinear multiphoton-absorption process, the modification occurs only at the focusing voxel, and we can form submicrometer-scaled 3D nanostructures with varying optical and magnetic properties.

Figure 1(a) shows a Ce:YIG wafer we used for the experiment. A 1.2-μm-thick magneto-optical single-crystalline Ce:YIG layer is grown on a (111)-oriented nonmagnetic garnet substrate [$(GdCa)_3(GaMgZr)_5O_{12}$ or SGGG] using magnetoron sputtering epitaxy with a substrate temperature of 690°C and an argon atmospheric pressure of 0.8 Pa. Figure 1(b) depicts the x-ray diffraction spectrum of the Ce:YIG/SGGG wafer. The spectrum shows very sharp Bragg reflections from a Ce:YIG(888) plane with clearly resolved $K\alpha 1$ and $K\alpha 2$ lines. The grown Ce:YIG layer had high crystallographic quality with a narrow half-linewidth of x-ray diffraction. The layer had a mirror-like surface with a yellowish green color and a relative refractive index of 2.2. It exhibited a weak coercive force of 30 Oe.

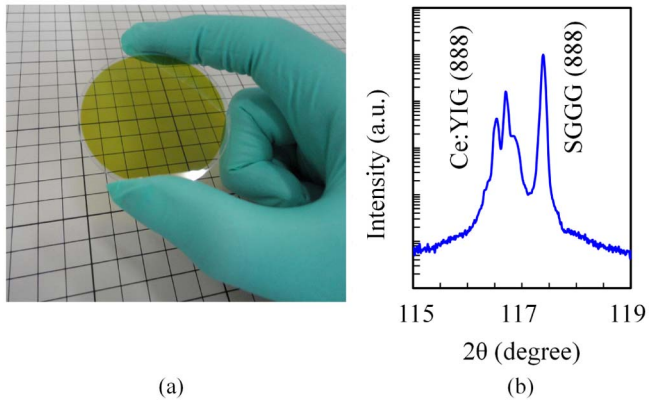

Fig. 1. (a) Epitaxial ferrimagnetic Ce:YIG layer grown on a (111)-oriented nonmagnetic garnet (SGGG) substrate. (b) X-ray diffraction spectrum of the Ce:YIG/SGGG wafer.

Figure 2 shows the optical system used for direct laser writing. The light source was a mode-locked Ti:sapphire laser with an 800 nm wavelength, 80 fs pulse width, and 82 MHz repetition rate. The laser beam was focused in the Ce:YIG layer, using an objective lens with a numerical aperture of 0.9, so that the multiphoton absorption would occur at the focusing voxel in the Ce:YIG layer. The Ce:YIG/SGGG shows no remarkable absorption at around the laser wavelength of 800 nm and shows a sharp increase in absorption at 400 nm or less. This shows that the effect of laser irradiation occurs only at a focal spot where the photon density is high enough to induce multiphoton absorption. The wafer was supported by an x–y stage and scanned in three dimensions using computer control. We observed the laser-written patterns from the backside (SGGG side) of the wafer during the irradiation process.

Using this system, we wrote patterns in the Ce:YIG layer. Figure 3(a) shows the line patterns observed with reflected light optical microscopy, and Fig. 3(b) shows the same sample observed with phase-contrast microscopy. In this example, we wrote five single-pass lines 1–5 with different laser powers and a multipass line 6 consisting of 20 single-pass lines. The laser power ranged from 30–76.5 mW at the entrance pupil of the objective for the five single-pass lines and was held at 48 mW for the multipass line. The scanning speed of the laser beam was set to 100 μm/min. We found that a laser power of 60 mW or higher caused thermal cracks to the Ce:YIG layer. This is shown in Fig. 3(a) by the two black stripes and in Fig. 3(b) by the two yellow stripes. At moderate powers, the laser writing changed the optical property of Ce:YIG without any cracking, and this can be observed by two thin lines (3 and 4) in Fig. 3(b). The width of the line was 1.5 μm for 48 mW and 750 nm for 38 mW. For laser powers of 30 mW or lower, we were not able to discern any remarkable changes in the optical properties.

Laser irradiation changed the refractive index of the Ce:YIG layer. We measured the change by means of quantitative phase imaging (QPI). The QPI is a technology, based on optical interferometry, to measure the image (or map) of path-length shifts associated with the

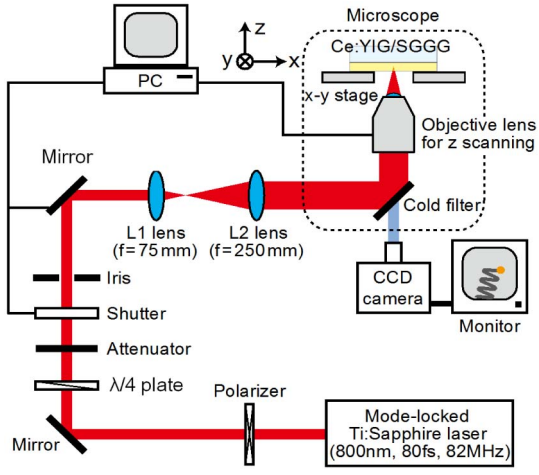

Fig. 2. Optical system used for direct 3D laser writing on a Ce:YIG layer grown on a SGGG substrate.

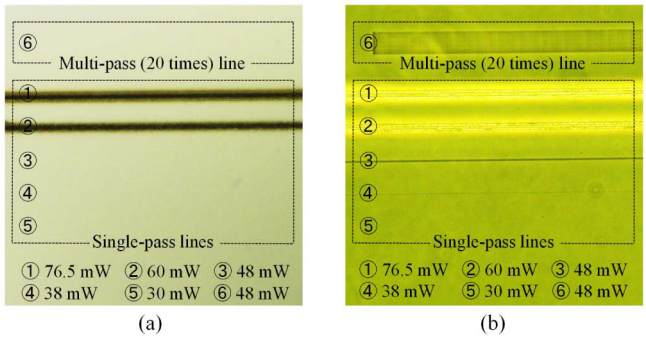

Fig. 3. Plane view of lines in Ce:YIG layer written with different laser powers, observed with (a) reflected light optical microscopy and (b) phase-contrast microscopy. One multipass line 6 and five single-pass lines 1–5 are written, but some of them cannot be observed (see text).

specimen. This image contains quantitative information about both the local thickness and refractive index of the structure. By comparing QPI information for the laser-irradiated Ce:YIG specimen with that for a nonirradiated Ce:YIG reference, we obtained knowledge about the intracrystal refractive index of the irradiated Ce:YIG. For the method, see [17] and [18]. The refractive index and the thickness of the nonirradiated Ce:YIG was measured beforehand with an ellipsometer and SEM. Figure 4(a) shows the profile of the changes around the laser-written lines. Laser irradiation increased the refractive index of the Ce:YIG layer. The increment, measured at a wavelength of 632.8 nm, was 0.015 ± 0.001 (0.7% of Ce:YIG refractive index) for the line created with a 48-mW laser power and 100 μm/min scanning speed [see Fig. 4(b)].

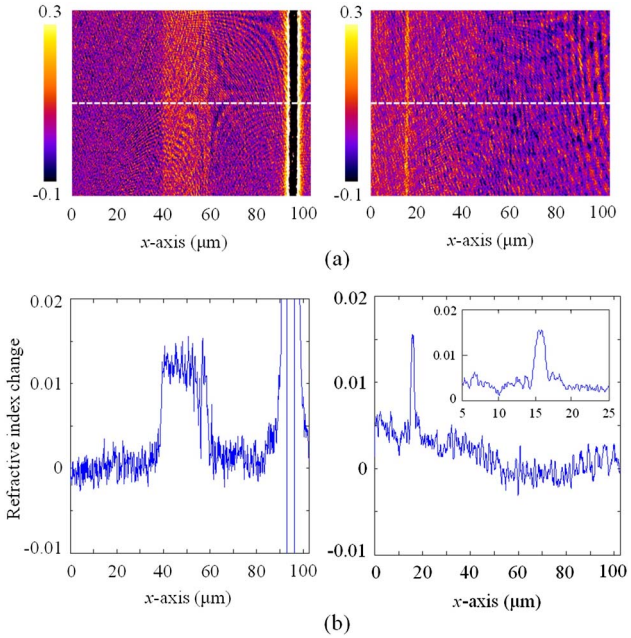

Fig. 4. Change in refractive index around irradiated Ce:YIG lines. (a) Distribution of change observed with quantitative phase imaging. The left profile is for lines 6 and 1 shown in Fig. 3, and the right profile is for lines 4 and 5. (b) Change in refractive index along the dashed lines in (a). The inset shows enlarged view of the data around the line 4.

The inset in Fig. 4(b) is the enlarged view of the refractive index profile around line 4. The edge-transition width of the line is less than 500 nm. To form an optical waveguide in the Ce:YIG with the refractive index change of 0.7%, a waveguide width has to be 10 μm or more for sufficient optical confinement. The edge-transition width is far smaller than the waveguide width and therefore does not affect the properties of the waveguide.

A significant goal in this study is to show that, unlike other transparent materials such as glasses and polymers, it is possible to control both the magnetic properties and the refractive index of the Ce:YIG layer. To confirm this, we measured the effect of laser irradiation on the magnetization of the Ce:YIG layer.

To see the magnetic-domain configuration in the Ce:YIG layer, we made use of the magneto-optical polar Kerr effect (MOKE). Figures 5(a)–5(c) show the MOKE images measured for a sample of Ce:YIG layer with laser-written lines. For reference, Fig. 5(d) shows a phase-contrast microscope image of the same sample. The MOKE images were taken using light from a mercury lamp at room temperature with an external magnetic field (parallel to the surface layer). The dark regions are positively magnetized, and the light regions are negatively magnetized.

First, we measured the sample with increasing the magnetic field from −500 to 500 Oe. At an external magnetic field of −470.7 Oe, the entire Ce:YIG layer was negatively magnetized [Fig. 5(a)]. Thus, the Ce:YIG layer, including irradiated regions, was magnetized in the same direction as the magnetic field. As magnetic field increased in the positive direction, the MOKE images changed, as shown in Figs. 5(b) and 5(c). The irradiated regions easily changed their magnetization in response to the external magnetic field. (The upper two lines are ignored because they are dislocated regions with cracks.) In contrast, the nonirradiated regions tended to maintain their magnetization. At an external magnetic field of 495 Oe, the entire Ce:YIG layer was positively magnetized [Fig. 5(d)]. After that, we measured the layer with sweeping the magnetic field from the positive side (500 Oe) to the negative side (−500 Oe) and observed that the domain showed a hysteretic cycling as shown in Figs. 5(e) and 5(f).

Figure 5(h) shows the schematic magnetization (M-H) curve of the Ce:YIG layer calculated from the measured domain configurations. The blue curve is for the irradiated region, and the red curve is for the nonirradiated region (This M-H curve is given simply to assist the understanding of the magnetic properties measured with MOKE imaging. More precisely, it is necessary to measure the magnetization curve for local nanometer regions.) Points (a)–(f) on the curves correspond to MOKE images (a)–(f), respectively. The laser irradiation changes the magnetic property of the Ce:YIG layer from hard to soft. In this way, we can achieve local control of the magnetization inside the Ce:YIG layer using laser irradiation.

These results show the usefulness of direct laser writing into Ce:YIG and other magneto-optical materials. In Fig. 6, we discuss two probable applications of laser writing for Ce:YIG. A nonreciprocal-phase-shift waveguide [19] can be formed in the Ce:YIG layer as shown in

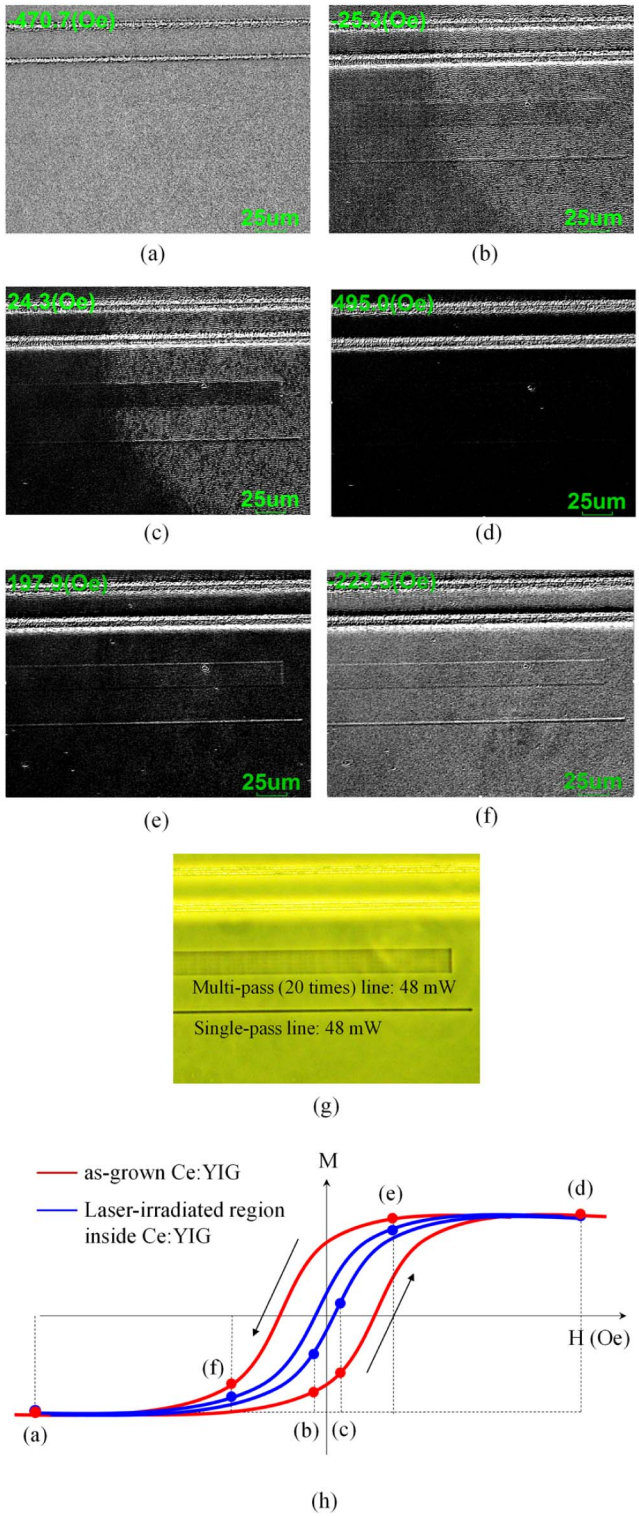

Fig. 5. Effect of laser irradiation on magnetization. (a)–(f) Magneto-optical polar-Kerr-effect images of the sample at room temperature. The dark regions are positively magnetized, and the light regions are negatively magnetized. Each figure shows the domain configurations under an external magnetic field of (a) −470.7 Oe, (b) −25.3 Oe, (c) 24.3 Oe, (d) 495 Oe, (e) 197.9 Oe, and (f) −223.5 Oe. (g) Phase-contrast microscope image of the same sample. (h) Schematic magnetization curve of Ce:YIG layer with and without irradiation.

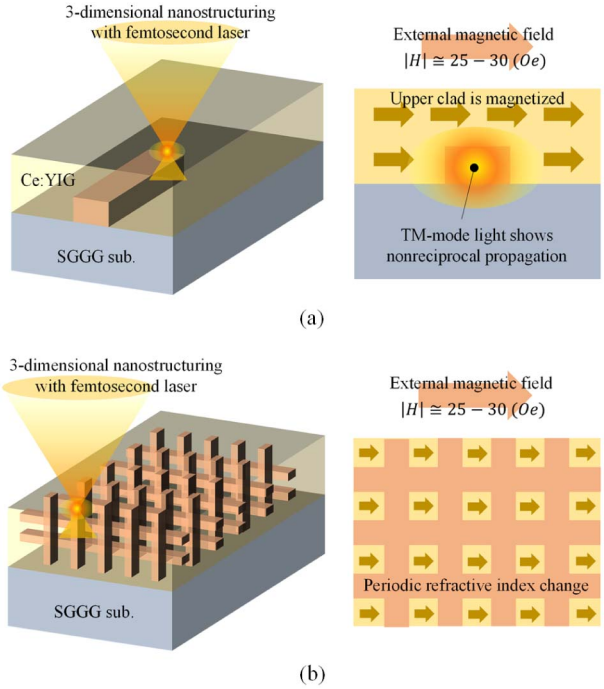

Fig. 6. Functional nanostructures formed monolithically inside Ce:YIG layer on SGGG substrate: (a) nonreciprocal-phase-shift waveguide and (b) 3D magneto-photonic crystal (or periodic nanostructure).

Fig. 6(a). A laser-irradiated stripline (waveguide) is formed inside the Ce:YIG layer at the interface between the Ce:YIG layer and the substrate. The upper cladding layer on the waveguide is left nonirradiated and therefore has a large residual magnetization. The resultant device is a nonreciprocal-phase-shift waveguide formed monolithically in the Ce:YIG layer. As an enhanced version of this device, we can make a waveguide optical isolator simply by writing waveguides into the Ce:YIG layer, forming a Mach–Zehnder interferometer.

A magneto-photonic crystal [20] can be made by writing a 3D nanostructure to form a spatially periodic refractive-index change inside the Ce:YIG, as shown in Fig. 6(b). The magnetization can be controlled space-periodically with an appropriate external magnetic field. Consequently, we can make a periodic optical and magnetic nanostructure in the Ce:YIG layer. With this magneto-photonic crystal, we will be able to achieve more flexible band engineering than in conventional photonic crystals.

As we have shown, laser irradiation can alter both the refractive index and magnetization of the Ce:YIG layer. The laser irradiation increases the refractive index by about 0.7% and changes the magnetic properties from hard to soft. Magneto-optical elements combined with optical waveguides can be formed monolithically in YIG. This technology will open new fields in the technology of YIG devices and contribute to the development of magneto-optical devices for optical communication and photonic integration.

This work was supported in part by the Ministry of Education, Culture, Sports, Science and Technology (MEXT); JSPS KAKENHI Grant Nos. 24246061, 24656046, 25420321, 22109006, 23710160, 24760270, 23000010, 24686040, and the Strategic Information and Communications R&D Promotion Programme (SCOPE) of the Ministry of Internal Affairs and Communications.

References

1. T. Boudiar, B. Payet-Gervy, M.-F. Blanc-Mignon, J.-J. Rousseau, M. Le Berre, and H. Joisten, J. Magn. Magn. Mater. **284**, 77 (2004).
2. M. C. Sekhar, J. Y. Hwang, M. Ferrera, Y. Linzon, L. Razzari, C. Harnagea, M. Zaezjev, A. Pignolet, and R. Morandotti, Appl. Phys. Lett. **94**, 181916 (2009).
3. A. K. Zvezdin and V. A. Kotov, *Modern Magnetooptics and Magnetooptical Materials* (Taylor & Francis, 1997).
4. H. Dötsch, N. Bahlmann, O. Zhuromskyy, M. Hammer, L. Wilkens, R. Gerhardt, P. Hertel, and A. F. Popkov, J. Opt. Soc. Am. B **22**, 240 (2005).
5. T. Mizumoto, R. Takei, and Y. Shoji, IEEE J. Quantum Electron. **48**, 252 (2012).
6. R. L. Espinola, T. Izuhara, M. C. Tsai, R. M. Osgood, Jr., and H. Dötsch, Opt. Lett. **29**, 941 (2004).
7. Y. Shoji, T. Mizumoto, H. Yokoi, I.-W. Hsieh, and R. M. Osgood, Jr., Appl. Phys. Lett. **92**, 071117 (2008).
8. M.-C. Tien, T. Mizumoto, P. Pintus, H. Kromer, and J. E. Bowers, Opt. Express **19**, 11740 (2011).
9. L. Bi, J. Hu, P. Jiang, D. H. Kim, G. F. Dionne, L. C. Kimerling, and C. A. Ross, Nat. Photonics **5**, 758 (2011).
10. S. Ghosh, S. Keyvaninia, Y. Shirato, T. Mizumoto, G. Roelkens, and R. Baets, IEEE Photon. J. **5**, 6601108 (2013).
11. R. Takei, K. Yoshida, and T. Mizumoto, Jpn. J. Appl. Phys. **49**, 086204 (2010).
12. K. M. Davis, K. Miura, N. Sugimoto, and K. Hirao, Opt. Lett. **21**, 1729 (1996).
13. C. B. Schaffer, A. Brodeur, J. F. Garcia, and E. Mazur, Opt. Lett. **26**, 93 (2001).
14. S. Nolte, M. Will, J. Burghoff, and A. Tuennermann, Appl. Phys. A **77**, 109 (2003).
15. S. L. Chin, S. A. Hosseini, W. Liu, Q. Luo, F. Théberge, N. Aközbek, A. Becker, V. P. Kandidov, O. G. Kosareva, and H. Schroeder, Can. J. Phys. **83**, 863 (2005).
16. T. Tanaka, A. Ishikawa, and S. Kawata, Appl. Phys. Lett. **88**, 081107 (2006).
17. H. Iwai, C. Fang-Yen, G. Popescu, A. Wax, K. Badizadegan, R. R. Dasari, and M. S. Feld, Opt. Lett. **29**, 2399 (2004).
18. T. Yamauchi, H. Iwai, M. Miwa, and Y. Yamashita, Opt. Express **16**, 12227 (2008).
19. H. Yokoi, T. Mizumoto, N. Shinjo, N. Futakuchi, and Y. Nakano, Appl. Opt. **39**, 6158 (2000).
20. I. L. Lyubchanskii, N. N. Dadoenkova, M. I. Lyubchanskii, E. A. Shapovalov, and Th. Rasing, J. Phys. D **36**, R277 (2003).